Corrosion Science xxx (2016) xxx–xxx

Contents lists available at ScienceDirect

Corrosion Science

journal homepage: www.elsevier.com/locate/corsci

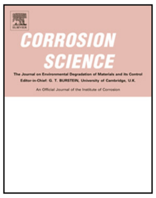

Investigation of the de-alloying behaviour of θ-phase (Al_2Cu) in AA2024-T351 aluminium alloy

X. Zhang, T. Hashimoto, J. Lindsay, X. Zhou*

Corrosion and Protection Centre, School of Materials, The University of Manchester, Manchester M13 9PL, UK, UK

ARTICLE INFO

Article history:
Received 10 January 2016
Received in revised form 4 March 2016
Accepted 5 March 2016
Available online xxx

Keywords:
A. Aluminium
A. Intermetallic
B. SEM
B. TEM
C. De-alloying

ABSTRACT

For multi-phase intermetallic particles consisting of both θ-and S-phase, de-alloying occurred preferentially at S-phase and the de-alloying of θ-phase initiated in the regions surrounding S-phase. The selective dissolution of Al from θ-phase resulted in porous copper-rich θ-phase remnant, comprised of randomly oriented copper metallic particles and copper oxides with sizes of 10–50 nm. Banding structure developed during the de-alloying of θ-phase particles that contain stacking faults. The de-alloying of θ-phase could preferentially occur from beneath the alloy surface, associated with the local low pH environment generated by trenching of the alloy matrix in the periphery θ-phase particles.

1. Introduction

AA2024 aluminium alloy has been widely used in aircraft industry due to its high strength-to-weight ratio and high damage tolerance. However, the high strength is achieved by the addition of relatively high content of copper as an alloying element, which may compromise corrosion resistance. It is known that the high corrosion susceptibility of copper-containing aluminium alloys is mainly attributed to the distribution of copper in the alloy, which enhances cathodic activity and, thereby, facilitates the development of localized corrosion [1–4]. It is believed that the de-alloying of copper-containing intermetallic particles, especially S-phase particles in AA2024 alloy, leads to copper re-distribution and, consequently, further enhances cathodic activity at the local sites. Thus, extensive work has been conducted to investigate the de-alloying behaviour of S-phase particles [2,5–11].

De-alloying is caused by the selective dissolution of more active alloying elements from a homogeneous phase [8,10,12]. A de-alloying model, considering the capillary effects during selective dissolution, was proposed by Sieradzki [10]. It was suggested that the preferential dissolution of more active alloying elements results in the regions of negative curvature on the alloy surface, which increases interfacial area and, consequently, increases the surface energy of the system. To achieve stability of the system, roughening transition, as a consequence of the competition between the curvature effect and the surface diffusion, occurs to decrease the surface energy of the system and, thereby, leads to the formation of the final stable surface morphology, namely porous structure, in the remnant. A continuum mode, based on the diffusive re-distribution of elements, has been proposed by Erlebacher, indicating that the intrinsic dynamical pattern formation process is responsible for the nano-porosity developed during the de-alloying process [8,13,14]. The application of the continuum model successfully predicts the characteristic length, i.e. average ligament size, of the de-alloyed remnant. It was also suggested that the curvature effect, which determines the average ligament size of the porous structure, governs the morphological evolution of de-alloying S-phase, whereas the balance between the metal dissolution, the ion solubility and the mass transport determines the kinetics of de-alloying process [5]. In addition to the theoretical work, the mechanism of porous structure formation during the de-alloying process of S-phase has also been proposed based on electron microscopy. Hashimoto et al. conducted a detailed investigation of the de-alloying behaviour of S-phase [11,15]. It was revealed that the de-alloying of S-phase produces the stable porous structure that consists of a modified S-phase network, copper nanoparticles at the intersections and a ~2 nm copper layer at the surface of the remnant, the latter prevents the occurrence of further de-alloying.

Although the de-alloying behaviour of synthetic θ-phase using atomic emission spectroelectrochemistry has been reported [16], the de-alloying mechanism of θ-phase particles in AA2024 alloy has attracted much less attention due to perhaps its less active nature

---

* Corresponding author.
E-mail address: xiaorong.zhou@manchester.ac.uk (X. Zhou).

http://dx.doi.org/10.1016/j.corsci.2016.03.003

Please cite this article in press as: X. Zhang, et al., Investigation of the de-alloying behaviour of θ-phase (Al_2Cu) in AA2024-T351 aluminium alloy, *Corros. Sci.* (2016), http://dx.doi.org/10.1016/j.corsci.2016.03.003

compared with S-phase particles. However, as a copper-containing intermetallic particle, the de-alloying of θ-phase also contributes to the copper re-distribution on the alloy surface and, consequently, affects the corrosion resistance of AA2024 alloy. Therefore, a comprehensive understanding of the de-alloying behaviour of θ-phase is necessary. In the present work, the de-alloying behaviour of θ-phase in AA2024-T351 aluminium alloy in a 3.5 wt.% NaCl solution has been investigated. Scanning and transmission electron microscopy are employed to investigate the evolution of morphology, composition and crystallographic structure of θ-phase during the de-alloying process.

2. Experimental methods

A 1.2 mm thick AA2024-T351 aluminium alloy sheet was used in the present study. The composition of the alloy was determined by inductively coupled plasma-atomic emission spectroscopy as following: Cu 4.65 wt.%; Fe 0.21 wt.%; Mg 1.54 wt.%; Mn 0.52 wt.%; Si 0.088 wt.%; Zn 0.11 wt.%; Al rem.

Prior to the corrosion testing, specimens were mechanically ground with 600, 1200, 2500 and 4000 grit silicon carbide paper and then polished sequentially with 3 μm and 1 μm diamond paste with mecaprex polishing liquid as lubricant. Following the mechanical polishing, the specimens were agitated ultrasonically in acetone bath for degreasing, rinsed in deionized water and dried in a cold air stream.

Corrosion testing was carried out by immersion in a 3.5 wt.% NaCl solution at ambient temperature. Before and after the testing, the alloy surface was examined with scanning electron microscopy (SEM) equipped with energy dispersive X-ray analysis (EDX). To avoid the influence of carbon deposit introduced during the SEM examination on the subsequent testing, the specimen was gently polished by colloidal silica suspension for a few seconds before corrosion testing. Electron transparent thin foils of the as-received AA2024 alloy were prepared with twin-jet electropolishing using a mixture of 700 ml methanol and 300 ml nitric acid at the temperature of −35 °C for transmission electron microscopy (TEM). In addition, focussed ion beam (FIB) was employed to obtain the electron transparent foils of de-alloyed θ-phase particles for TEM examination.

3. Results

3.1. The distribution of intermetallic particles

A mechanically polished specimen of the AA2024 alloy was examined to determine the distribution and composition of intermetallic particles. Fig. 1 (a) shows the backscattered electron micrograph of the randomly distributed intermetallic particles of micrometre size, appearing as bright features, on the alloy surface. EDX analysis was performed on the intermetallic particles, revealing three different types of intermetallic particles based on the compositions. They are S-phase that is rich in aluminium, copper and magnesium, θ-phase that is rich in aluminium and copper as well as α-phase that is rich in aluminium, copper, iron, manganese and silicon.

As shown in Fig. 1 (b, c), SEM micrographs at increased magnifications reveal that θ-phase particles are present individually or embedded with S-phase particles. Specially, a multi-phase particle, with a θ-phase outer shell and an S-phase inner core, is evident in Fig. 1 (c). Fig. 1 (d) exhibits the backscattered electron micrograph of another multi-phase particle, also consisting of S-phase and θ-phase, as confirmed by the corresponding EDX maps (Fig. 1 (e)). It is evident that two individual S-phase particles with the diameters of ∼400 nm are embedded in a θ-phase particle with the dimension of ∼3 μm.

The twin-jet electropolished thin foil of the AA2024 alloy was examined with TEM. A bright field TEM micrograph, as shown in Fig. 2 (a), displays a θ-phase particle decorated by several parallel linear features. The linear features are the stacking faults in θ-phase particles (confirmed by lattice image in the following section). The distances between the neighbouring linear features range from tens of nanometres to several hundred nanometres. The corresponding diffraction pattern is displayed in Fig. 2 (b), suggesting that the stacking faults are on the {011} planes of θ-phase. Two further examples of linear features in θ-phase particles are shown in Fig. 2 (c, d).

3.2. Morphological evolution of θ-phase particles

In order to examine the morphological modification of θ-phase during immersion in a 3.5 wt.% NaCl solution, SEM was carried out before and after the immersion. Fig. 3 (a) shows the SEM micrograph of a typical surface region containing intermetallic particles before the immersion testing. Particle 1, as marked in Fig. 3 (a), was selected for further analysis. EDX analysis of Particle 1 (Table 1) reveals Al and Cu, consistent with that of θ-phase. Fig. 3 (b) displays the SEM micrograph of Particle 1 after the immersion in a 3.5 wt.% NaCl solution for 30 min. It is evident that a gap, i.e. trenching, with the width of approximate 200 nm developed in the periphery of the θ-phase particle, suggesting the preferential dissolution of the alloy matrix.

The compositions of Particle 1 and the alloy matrix are compared before and after the immersion testing, as presented in Table 1. The increased oxygen contents on the particle and the alloy matrix suggests the presence of corrosion product after the immersion. It is also evident that the oxygen content of the particle is significantly higher than that of the alloy matrix, suggesting that localized corrosion preferentially occurred in the region containing θ-phase particles due to the increased electrochemical activity. Since the presence of oxygen changed the relative elemental percentage of copper and aluminium in the EDX analysis, the ratios of Cu/Al were also included in Table 1 to evaluate the compositional modification of the θ-phase particle. It is evident that, after the immersion, the ratio of Cu/Al of Particle 1 increased significantly from 0.69 to 1.56, suggesting the enrichment of copper in the θ-phase remnant. Previous work [2,3,11,17] suggested two possible explanations for the copper rich nature of the θ-phase remnant. First, copper ions generated by the dissolution of the alloy matrix re-deposited on the cathodic θ-phase particle. Second, the copper enrichment was the consequence of selective dissolution of Al from the θ-phase particle. However, as shown in Fig. 3 (b), no deposited particles were present on the θ-phase particle remnant after the immersion. Hence, it is likely that the selective dissolution of aluminium from the θ-phase particle is responsible for the copper rich nature of the remnant, which will be further elucidated in the following sections.

Fig. 4 displays the typical morphologies of θ-phase particles after immersion in a 3.5 wt.% NaCl solution for 10 h. It is evident that trenching was present between the θ-phase particle remnants and the peripheral alloy matrix, consistent with the morphology shown in Fig. 3 (b). In addition to trenching, some other characteristic features had also developed. Two typical θ-phase particles are shown in Fig. 4 (a, b), with pits of ∼2 μm dimensions within the particles, as indicated by the arrows. It is noticed that the dimensions of the pits are consistent with those of the S-phase particles embedded in the θ-phase particles (Fig. 1 (e, f)), suggesting that the development of the pit might be associated with the S-phase particle, i.e. the preferential attack of the relatively active S-phase resulted in the pits. Fig. 4 (c, d) shows further evidences of preferential attack of S-phase embedded in the θ-phase particle. In addition to the pits

Please cite this article in press as: X. Zhang, et al., Investigation of the de-alloying behaviour of θ-phase (Al_2Cu) in AA2024-T351 aluminium alloy, *Corros. Sci.* (2016), http://dx.doi.org/10.1016/j.corsci.2016.03.003